Comparison of Multiview Echocardiography Fusion Using Traditional and Deep Learning Models

Sharanya Balachandran[1,2], Michelle Noga[1,2], Harald Becher[3], Jonathan Windram[3], Pierre Boulanger[4] and Kumaradevan Punithakumar[1,2]
[1] Radiology and Diagnostic Imaging, University of Alberta, Edmonton, Canada
[2] Servier Virtual Cardiac Centre, Mazankowski Alberta Heart Institute, Edmonton, Canada
[3] Division of Cardiology, Mazankowski Heart Institute, University of Alberta, Edmonton, Canada
[4] Computing Science, University of Alberta, Edmonton, Canada
Email: balachan@ualberta.ca

INTRODUCTION

Cardiovascular disease is Canada's second leading cause of death. Echocardiography is one of the preferred ways of examining cardiovascular diseases as it is cost-effective and easy to use. However, echo scans suffer from a low signal-to-noise ratio and occasional signal dropout. These limitations can be overcome by developing an image fusion process that combines more than two images from multiple views of the heart, to increase the information and quality of the images.

MATERIALS AND METHODS

A deep learning-based cardiac image fusion is proposed using U-Net [1], which is trained as an auto-encoder feeding the cardiac images from different views and generate fused image. Other networks, DenseFuse [2] originally used for natural image fusion, ACU^{2}E-Net [3] originally proposed for thyroid lobe segmentation, and the fusion network modeled for multi-modal, multi-exposure, and multi-focus images called U2Fusion [4] is adopted for cardiac image fusion.

The ultrasound images were captured from different acoustic windows, typically apical and parasternal, using an X5 probe on a Philips EPIQ 7C scanner. The ultrasonic transducer was mounted on a Universal Robots UR10e arm, which facilitated its control during scanning. The models are executed on total of 13 volunteer dataset including 19440 two-dimensional (2D) slices for training, 11160 2D slices for validation, and 6030 2D slices for testing. Quality metrics including Peak Signal-to-Noise ratio (PSNR), entropy, and Structural Similarity (SSIM) are used for benchmarking the traditional and deep-learning methods.

RESULTS AND DISCUSSION

The proposed deep learning method eliminates the need to extract hand-crafted features used in traditional fusion, thus allowing a higher-quality fusion result. The U2Fusion model outperforms other methods both quantitatively as shown in Table 1 and qualitatively as shown in Fig 1.

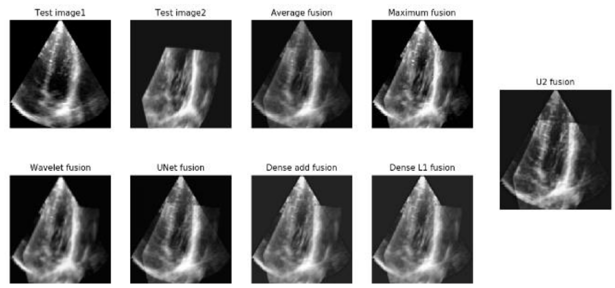

Fig 1 Qualitative comparison of fusion results.

CONCLUSIONS

The study demonstrated the benefits of using neural networks to fuse 2D images. The clinical significance of this network is assisting in the accurate visualization of the focus regions of heart structures, including vital information such as the edges of the chambers.

REFERENCES

[1] O. Ronneberger, P. Fischer, and T. Brox, "U-Net: Convolutional Networks for Biomedical Image Segmentation." arXiv, May 2015.
[2] H. Li and X.-J. Wu, "DenseFuse: A Fusion Approach to Infrared and Visible Images," IEEE Trans. Image Process., vol. 28, no. 5, pp. 2614–2623, May 2019.
[3] Balachandran, S et.al., "ACU2E-Net: A novel predict–refine attention network for segmentation of soft-tissue structures in ultrasound images", Computers In Biology And Medicine, vol. 157, March 2023.
[4] H. Xu et al., "U2Fusion: A Unified Unsupervised Image Fusion Network," IEEE Transactions on Pattern Analysis and Machine Intelligence, Jan 2022.

Table 1: Quantitative comparison of fusion results using quality metrics

Methods	PSNR (↑)	SSIM (↑)	Entropy (↑)	CNR (↑)
Average fusion	21.88 ± 1.87	0.52 ± 0.07	5.26 ± 0.13	0.49 ± 0.06
Maximum fusion	29.95 ± 1.54	0.59 ± 0.06	4.92 ± 0.21	0.61 ± 0.05
Wavelet fusion	28.86 ± 1.69	0.56 ± 0.07	5.13 ±0.17	0.61 ± 0.04
U-Net fusion	23.29 ± 2.06	0.57 ± 0.05	5.35 ± 0.20	0.51 ± 0.07
DenseFuse – L1 norm	21.82 ± 1.86	0.53 ± 0.07	5.35 ± 0.17	0.51 ± 0.07
DenseFuse – Addition	21.67 ± 1.89	0.52 ± 0.07	5.33 ± 0.18	0.53 ± 0.04
ACU^{2}E-Net fusion	20.36 ± 1.96	0.42 ± 0.07	3.86 ± 0.25	0.35 ± 0.07
U2Fusion	**30.18 ± 1.66**	**0.60 ±0.04**	**5.68 ± 0.17**	**0.66 ± 0.04**